The effects of resonant magnetic perturbations on fast ion confinement in the Mega Amp Spherical Tokamak

K.G. McClements[1], R.J. Akers[1], W.U. Boeglin[2], M. Cecconello[3], D. Keeling[1], O.M. Jones[1,4], A. Kirk[1], I. Klimek[3], R.V. Perez[2], K. Shinohara[5], K. Tani[6]

[1] *CCFE, Culham Science Centre, Abingdon, Oxfordshire, OX14 3DB, UK*

[2] *Department of Physics, Florida International University, Miami, Florida 33199, USA*

[3] *Department of Physics and Astronomy, Uppsala University, SE-751 05, Uppsala, Sweden*

[4] *Department of Physics, Durham University, South Road, Durham DH1 3LE, UK*

[5] *Japan Atomic Energy Agency, Naka, Ibaraki 311-0193, Japan*

[6] *Tokyo Institute of Technology, 2-12-1 Ookayama, Meguro-ku, Tokyo 152-8550, Japan*

1. Introduction

Resonant magnetic perturbations (RMPs) are frequently superimposed on the axisymmetric fields in tokamak plasmas to suppress or ameliorate edge localised modes (ELMs). In several devices RMPs have been found to degrade energetic ion confinement [1-3]. In this paper we report evidence for RMP-induced beam ion transport in the Mega Amp Spherical Tokamak (MAST); further details can be found in [4].

2. Experimental evidence for RMP-induced fast ion transport in MAST

Fig. 1 shows time traces from two single-null diverted (SND), MAST pulses with plasma current I_p = 400kA: 30086 (RMPs with toroidal mode number n = 3) and 30090 (no RMPs). The application of RMPs coincided with a substantial drop in total neutron rate S_n that was not matched in pulse 30090, which had no RMPs. As was usual in MAST, the application of RMPs caused the ELMs to have somewhat lower amplitudes and to occur more frequently [Fig. 1(c)]. The NUBEAM module of the TRANSP plasma simulation code is used to model the collisional evolution of beam ions, with the option of adding *ad hoc* non-collisional transport [5]. Fig. 2(a) again shows S_n in pulse 30086 (black curve), here with synthetic rates computed from NUBEAM simulations with purely collisional transport (green dashed-dotted curve) and with additional diffusivity D_a = 1m^{2}s^{-1} (blue dotted curve). The synthetic rate from the simulation with anomalous fast ion transport tracks the measured rate fairly well until RMPs are applied, then remains high while the measured rate drops by nearly 50%. Shortly after the application of RMPs in 30086, the amplitude of MHD activity

dropped considerably [Fig 2(b)], which suggests that it would be appropriate to set $D_a = 0$ during this phase of the pulse, were it not for the presence of RMP-induced transport.

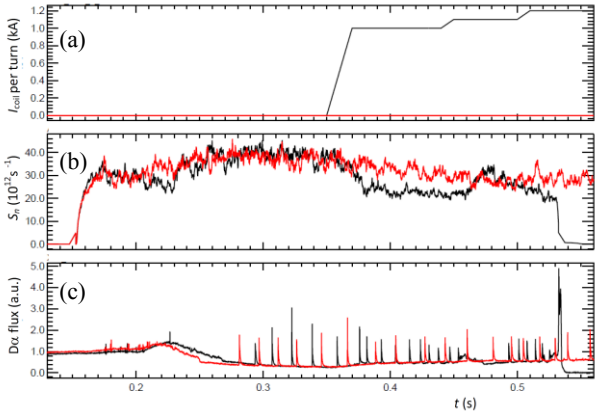

Fig. 1 Time traces from MAST pulses 30086 (black) and 30090 (red) showing (a) RMP coil current per turn, (b) neutron rate S_n, and (c) Dα emission.

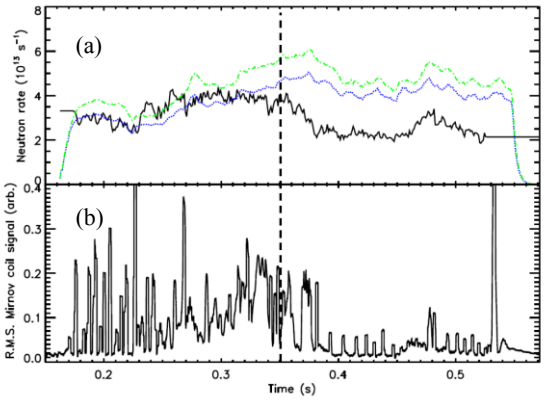

Fig. 2 (a) Measured neutron rate (black) and rates simulated using TRANSP with $D_a = 0$ (green curve) and $D_a = 1\text{m}^2\text{s}^{-1}$ (blue curve) in MAST pulse 30086. (b) Root mean square signal measured using outboard Mirnov coil. The dashed vertical line indicates the time at which RMPs were first applied.

Fig. 3 shows rates of fusion protons recorded in four channels, corresponding to unconfined particle trajectories crossing the midplane at four different major radii (indicated on the figure) for pulse 30086. A similar trend can be seen in all channels and in S_n, with drops in the measured rates occurring shortly after the end of the RMP ramp-up.

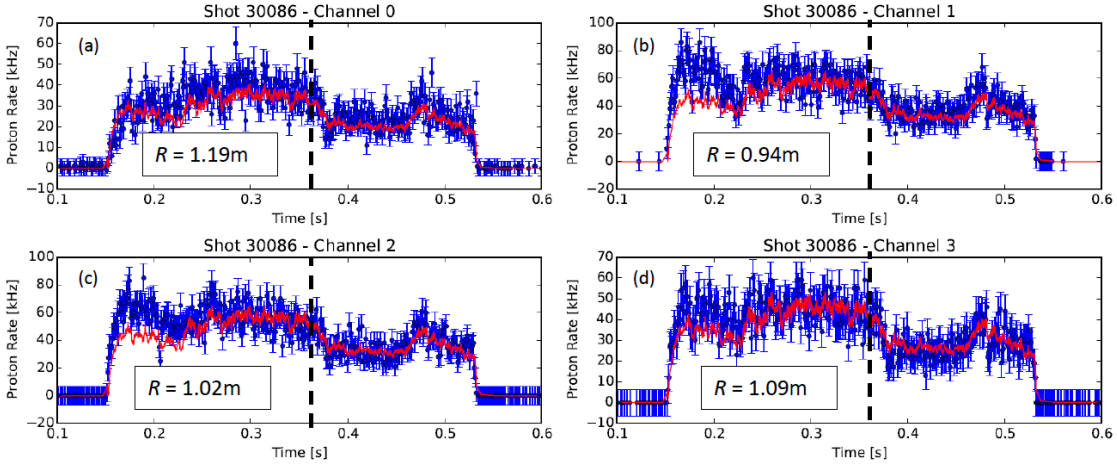

Fig. 3 Blue circles: rates of fusion protons recorded in four detector channels during MAST pulse 30086. Red curves: S_n normalised to same scale as proton rates. The dashed lines indicate the time at which the RMP coil current reached its maximum value. The values of R are the average major radii at which protons detected in the four channels crossed the midplane.

Fig. 4 shows fast ion Dα (FIDA) emission in the two pulses discussed above. The left-hand and right-hand plots show data for two different values of R, here representing the average major radius at which the FIDA line of sight intersected one of the beamlines. Higher Doppler shifts from the Dα rest wavelength in air (656.1 nm) correspond to higher

line-of-sight velocities, hence higher minimum beam ion energies, which are indicated on the figure. When the RMPs are applied the emission drops sharply at both values of R and in every wavelength range, suggesting that fast ions with a wide range of energies are affected.

Fig. 5 shows total neutron rates and neutron camera (NC) data from two similar pulses, with and without RMPs. In the former the RMP coil current was ramped up gradually then held constant [Fig 5(a)]. In Figs. 5(c-e) the parameter p is the tangency major radius of the NC line of sight while Z is the vertical position of the line of sight at the tangency point. The total neutron rates and the rates in all NC channels clearly diverge as the coil currents are ramped up, with many fewer neutrons being produced in the pulse with RMPs.

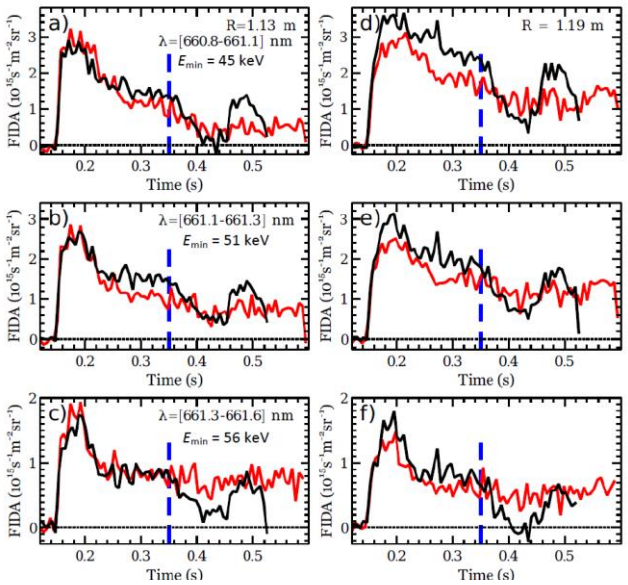

Fig. 4 FIDA emission versus time in MAST pulses 30086 (black) and 30090 (red) for three wavelength ranges, corresponding to different minimum fast ion energies, and two major radii, R. Dashed lines indicate the time at which RMPs were applied in pulse 30086.

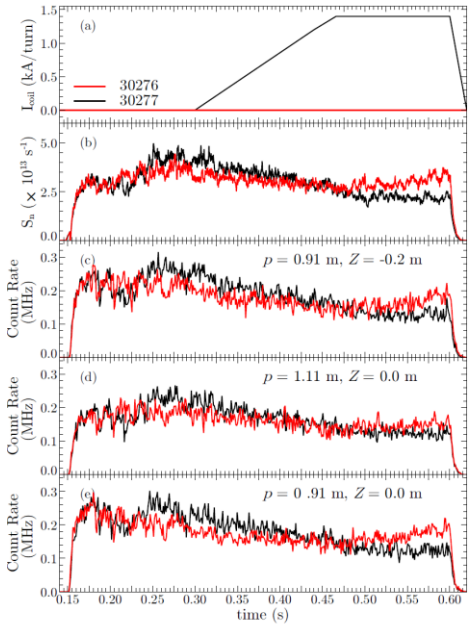

Fig. 5 Time traces from MAST pulses 30276 (red) and 30277 (black) showing (a) RMP coil current per turn, (b) S_n, and (c-e) neutron rates in three different NC channels.

3. First principles-based modelling

Simulations of beam ions in MAST plasmas with and without RMPs have been carried out using the F3D-OFMC code [6]. Beam ion orbits were tracked from birth to thermalization, taking into account collisions with bulk ions and electrons. The simulated RMPs had n = 6, and the equilibrium and plasma profiles were based on SND MAST pulse 27205, with I_p = 600 kA. Two alternative representations of the first wall (at which particles were considered to be lost) were used, designated as W1 and W2: see Fig. 6 in [4]. Both MAST neutral beams were modelled in the simulations, with primary birth energies set equal to 65 keV and 51 keV. Table 1 lists the figures obtained in the simulations for the total loss of neutral beam heating

power due to fast ion losses. It is apparent that the RMP-induced loss of beam heating power (~11%) does not depend on either the choice of first wall or finite Larmor radius effects.

magnetic field	orbit-following scheme	wall	Total loss of beam power (%)	loss of power due to RMPs (%)
axisymmetric	full orbit	W1	5.7	-
n = 6 RMPs	full orbit	W1	16.5	10.8
n = 6 RMPs	guiding centre	W1	16.2	10.5
axisymmetric	full orbit	W2	11.5	-
n = 6 RMPs	full orbit	W2	22.6	11.1
n = 6 RMPs	guiding centre	W2	22.1	10.6

Table 1. Beam power losses found in F3D-OFMC simulations of MAST plasmas. RMP-induced losses were obtained by subtracting results for full orbit losses in axisymmetric plasmas from total figures.

4. Summary

The effects of RMPs on beam ion confinement in MAST have been studied using measurements of neutrons, fusion protons and FIDA emission. In SND MAST pulses with I_p = 400 kA, the total neutron emission dropped by around a factor of two when n = 3 RMPs were applied. The measured neutron rate during RMPs was much lower than that calculated using TRANSP, even when non-classical (but axisymmetric) *ad hoc* fast ion transport was taken into account. Sharp drops in spatially-resolved neutron rates, fusion proton rates and FIDA emission were also observed. First principles-based simulations of RMP-induced fast ion transport in MAST, using the F3D-OFMC code, show similar losses for two alternative representations of the MAST first wall, with and without full orbit effects taken into account; for n = 6 RMPs in a 600 kA plasma, the additional loss of beam power due to the RMPs was found in the simulations to be approximately 11%.

This work has received funding from the RCUK Energy Programme [grant number EP/I501045] and from Euratom. The views and opinions expressed herein do not necessarily reflect those of the European Commission.

[1] M. Garcia-Munoz et al., Plasma Phys. Control. Fusion **55**, 124014 (2013)

[2] M. Garcia-Munoz et al., Nucl. Fusion **53**, 123008 (2013)

[3] M.A. Van Zeeland et al, Plasma Phys. Control. Fusion **56**, 015009 (2014)

[4] K.G. McClements et al., Plasma Phys. Control. Fusion **57**, 075003 (2015)

[5] A. Pankin et al., Comput. Phys. Commun. **159**, 157 (2004)

[6] K. Tani et al., J. Phys. Soc. Japan **50**, 1726 (1981)